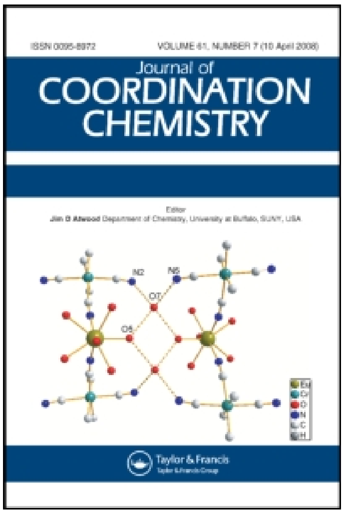

Journal of Coordination Chemistry

Publication details, including instructions for authors and subscription information:
http://www.informaworld.com/smpp/title~content=t713455674

Acetone salicyloylhydrazone of Ni(II): synthesis, molecular structures, and properties

Bei Liang[a]; Xiangrong Liu[a]; Jianjun Chen[a]; Kanshe Li[a]
[a] College of Chemistry and Chemical Engineering, Xi'an University of Science and Technology, Xi'an 710054, P.R. China

First published on: 25 June 2010

To cite this Article Liang, Bei , Liu, Xiangrong , Chen, Jianjun and Li, Kanshe(2010) 'Acetone salicyloylhydrazone of Ni(II): synthesis, molecular structures, and properties', Journal of Coordination Chemistry, 63: 11, 1951 — 1959, First published on: 25 June 2010 (iFirst)

To link to this Article: DOI: 10.1080/00958972.2010.495156

URL: http://dx.doi.org/10.1080/00958972.2010.495156

Journal of Coordination Chemistry
Vol. 63, No. 11, 10 June 2010, 1951–1959

Taylor & Francis
Taylor & Francis Group

Acetone salicyloylhydrazone of Ni(II): synthesis, molecular structures, and properties

BEI LIANG, XIANGRONG LIU*, JIANJUN CHEN and KANSHE LI

College of Chemistry and Chemical Engineering,
Xi'an University of Science and Technology, Xi'an 710054, P.R. China

(*Received 4 February 2010; in final form 16 March 2010*)

Two new mononuclear Ni(II) complexes, $[Ni(C_{10}H_{12}O_2N_2)_2(C_5H_5N)_2](NO_3)_2$ (**1**) and $[Ni(C_{10}H_{12}O_2N_2)_2(H_2O)_2](NO_3)_2$ (**2**), have been synthesized and characterized by elemental analysis, infrared, UV-Vis spectroscopy, and single-crystal X-ray diffraction. The coordination geometry around each Ni(II) can be described as an octahedron with each Ni(II) coordinated to two imino nitrogens, two carbonyl oxygens, and two solvent molecules (pyridine for **1** and water for **2**). In the synthesis, the original ligand changes from *o*-carboxybenzaldehyde salicyloylhydrazone ($C_{15}H_{12}O_4N_2$) into acetone salicyloylhydrazone ($C_{10}H_{12}O_2N_2$). The thermal stability of the complexes at three different heating rates ($\beta = 5$, 10, and $15^\circ C\,min^{-1}$) show that all the complexes exhibit three thermal decomposition stages and their thermal stability is **1** > **2**. Complexes **1** and **2** both display DNA binding ability, ascertained by UV-Vis titration.

Keywords: Synthesis; Molecular structure; Complex; Thermal stability; Catalytic activity

1. Introduction

Hydrazone has been extensively investigated during the past decades [1] mainly due to its ability to form complexes with different metal ions [2], with applications in biochemistry, agriculture, and catalysis [3–6]. The complexes usually have better properties than the ligands or metal ions [7]. There are some reports [8–10] that Ni(II) complexes can accelerate the cleavage of double-stranded DNA, while other Ni(II) complexes have excellent catalytic activity. The presence of pyridine groups in the complexes offers the possibility to obtain highly stable metal complexes [11].

This article investigates the structure–function relationships of the complexes of transition metal ions with hydrazones. The crystal structures of the complexes were determined and thermal decomposition behavior was investigated. We also investigated the catalytic decomposition activity of the compounds to hydrogen peroxide and the binding properties of the complexes with CT-DNA.

---

*Corresponding author. Email: xkchemistry@yahoo.com.cn

Journal of Coordination Chemistry
ISSN 0095-8972 print/ISSN 1029-0389 online © 2010 Taylor & Francis
DOI: 10.1080/00958972.2010.495156

2. Experimental

2.1. *Measurements*

Elemental analyses were carried out on a P.E.2400-II instrument. Infrared (IR) spectra were recorded on a P.E.983 FT-IR spectrophotometer with KBr pellets. UV-Vis spectra were obtained on a TU-1900 spectrophotometer in DMF at 10^{-5} M. The crystal structures of the complexes were determined using a Bruker SMART APEX CCD diffractometer equipped with graphite monochromated Mo-Kα radiation ($\lambda = 0.71073$ Å). Thermal data were collected on a Q1000DSC+LNCS+FACS Q600SDT instrument under nitrogen with three different heating rates of 5, 10, and 15°C min^{-1} from 30°C to 800°C.

2.2. *Preparation*

All chemicals were purchased commercially and used as received; the CT-DNA was purchased from Sigma company. The CT-DNA was dissolved in Tris buffer (0.1 mol L^{-1}, pH = 7.33) and its purity was checked from the absorbance ratio A260/A280. For all the solutions, this ratio was in the range of 1.8–1.9. $C_{15}H_{12}O_4N_2$ was prepared according to the literature method [12].

2.2.1. Synthesis of $[Ni(C_{10}H_{12}O_2N_2)_2(C_5H_5N)_2](NO_3)_2$ (1). A solution of $Ni(NO_3)_2 \cdot 6H_2O$ (0.12 g, 0.4 mmol) in C_5H_5N (7 mL) was added to a solution of $C_{15}H_{12}O_4N_2$ (0.24 g, 0.8 mmol) in DMF (5 mL). The mixture was stirred and heated at 50°C in a water bath for 1 h. The resulting solution was kept in acetone for slow evaporation at room temperature. After a week, purple crystals of $[Ni(C_{10}H_{12}O_2N_2)_2(C_5H_5N)_2](NO_3)_2$ were collected by filtration, washed with methanol and dried. Anal. Calcd for **1** (%): C, 49.68; H, 4.69; N, 15.45; O, 22.08. Found (%): C, 50.06; H, 5.01; N, 14.96; O, 23.05.

2.2.2. Synthesis of $[Ni(C_{10}H_{12}O_2N_2)_2(H_2O)_2](NO_3)_2$ (2). A solution of $Ni(NO_3)_2 \cdot 6H_2O$ (0.12 g, 0.4 mmol) in CH_3OH (7 mL) was added to a solution of $C_{15}H_{12}O_4N_2$ (0.24 g, 0.8 mmol) in DMF (5 mL). The resulting solution was heated at 50°C in a water bath for 1 h. Then the solution was left in acetone for slow evaporation at room temperature. After 2 weeks, blue crystals of $[Ni(C_{10}H_{12}O_2N_2)_2(H_2O)_2](NO_3)_2$ were collected by filtration, washed with methanol, and dried. Anal. Calcd for **2** (%): C, 39.82; H, 4.65; N, 13.94; O, 31.86. Found (%): C, 40.02; H, 4.73; N, 12.96; O, 32.21.

2.3. *X-ray crystal structure determination*

Data collection for **1** and **2** were performed at 293(2) K with graphite monochromated Mo-Kα radiation ($\lambda = 0.71073$ Å). The structures were solved by direct methods and refined by full-matrix least-squares on F^2 with the SHELXTL-97 program. The non-hydrogen atoms were located with difference Fourier synthesis and hydrogens were generated geometrically. Crystallographic information is summarized in table 1.

Table 1. Crystallographic information of **1** and **2**.

	1	**2**
Formula	$C_{30}H_{34}N_8NiO_{10}$	$C_{20}H_{28}N_6NiO_{12}$
Formula weight	725.34	603.17
Crystal color	Purple	Blue
Crystal system	Monoclinic	Monoclinic
Space group	*C2/c*	*P*2(1)/*n*
Unit cell dimensions (Å, °)		
a	20.059(5)	10.4113(11)
b	14.385(4)	10.2442(11)
c	15.792(7)	13.2109(13)
β	126.395	109.768(2)
Volume (Å^3), Z	3668(2), 4	1326.0(2), 2
Calculated density ($mg\,m^{-3}$)	1.314	1.511
Absorption coefficient (mm^{-1})	0.591	0.803
$F(000)$	1512	628
Crystal size (mm^3)	0.30 × 0.28 × 0.20	0.31 × 0.25 × 0.13
θ range (°)	1.90–26.30	2.17–25.09
Limiting indices	$-24 \le h \le 13$; $-16 \le k \le 17$; $-17 \le l \le 19$	$-12 \le h \le 10$; $-12 \le k \le 11$; $-15 \le l \le 15$
Reflections collected/unique	10015/3729	6486/2374
Data/restraints/parameters	[$R(\text{int}) = 0.0503$]	[$R(\text{int}) = 0.0295$]
Goodness of fit on F^2	3713/0/217	2374/0/189
R indices [$I > 2\sigma(I)$]	1.039	1.076
R indices (all data)	$R_1 = 0.0626$, $\omega R_2 = 0.1642$	$R_1 = 0.0366$, $\omega R_2 = 0.0902$
	0.1199, 0.2028	0.0525, 0.0977

2.4. *Decomposition of hydrogen peroxide*

A mixture of 1 mL ($1\,mol\,L^{-1}$) catalyst (**1**, **2**, ligand, or nickelous nitrate hexahydrate) and 20 mL (15%) hydrogen peroxide was put aside for 1 day (20°C), then titrated with potassium permanganate standard solution. From the titration data, the percentage of hydrogen peroxide decomposition was calculated.

3. Results and discussion

3.1. *Structures description*

The coordination modes are discerned in scheme 1. The crystal structures and the cell packing structures of **1** and **2** are shown in figures 1–4. Single crystal X-ray diffraction results show that both mononuclear complexes are formed around centers of symmetry. Selected bond lengths and angles are given in table 2. Hydrogen bonding geometry is given in table 3.

The environment around Ni(II) in **1** and **2** can be described as octahedral with the ligand–metal–ligand angles varying among 101.22(11)°(N1–Ni–O1), 178.98(14)° (N1–Ni–N1A), and 89.49(7)°(N3–Ni–N1) for **1** and 78.85(7)°(N1–Ni–O2), 180.00(11)°(N1–Ni–N1A), and 87.24(8)°(O1–Ni–N1) for **2**. In **1**, the Ni(II) is coordinated to two nitrogens (N3 and N4) of pyridine and two bidentate ligands. The bonds to Ni(II) through oxygen of carbonyl and nitrogen of imino form two, five-membered chelate rings. In **2**, the Ni(II) is coordinated to two bidentate ligands

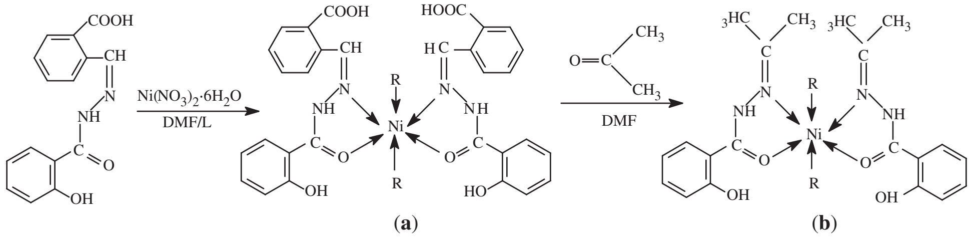

R=C_5H_5N, H_2O L=C_5H_5N, CH_3OH

Scheme 1. Formation of complexes.

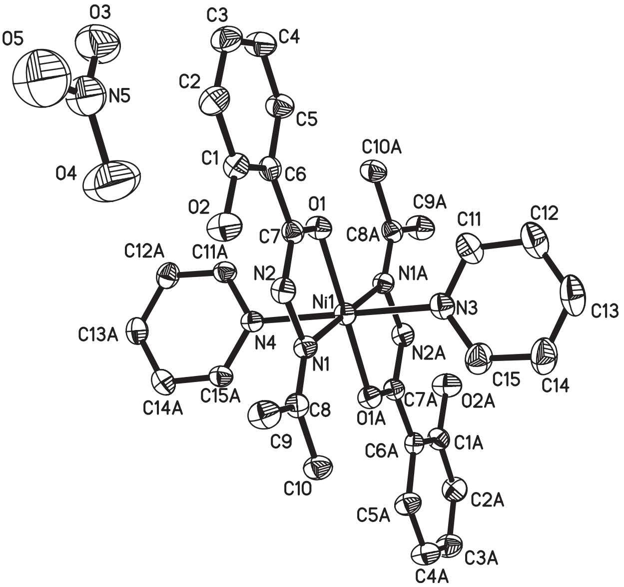

Figure 1. Crystal of **1**.

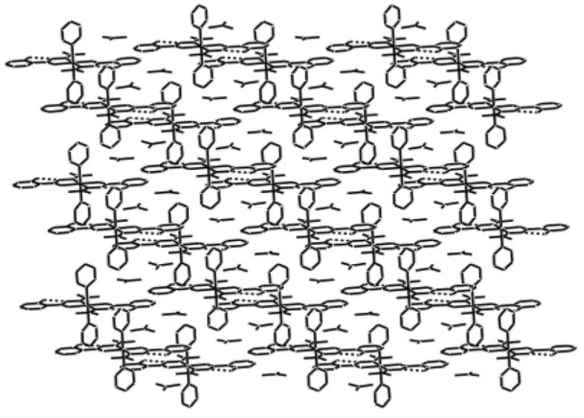

Figure 2. Cell packing of **1**.

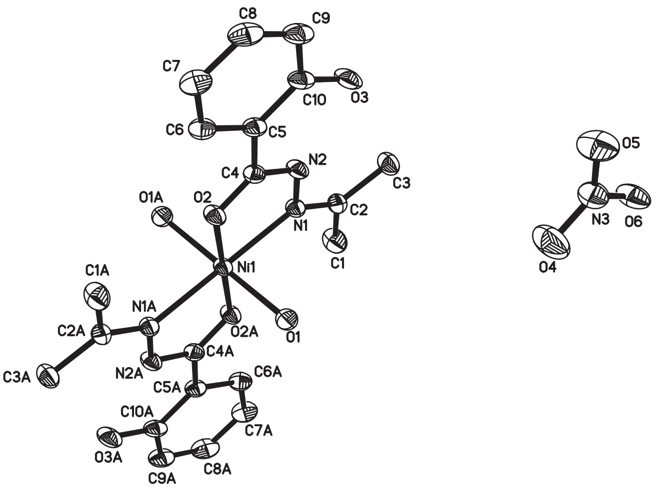

Figure 3. Crystal of **2**.

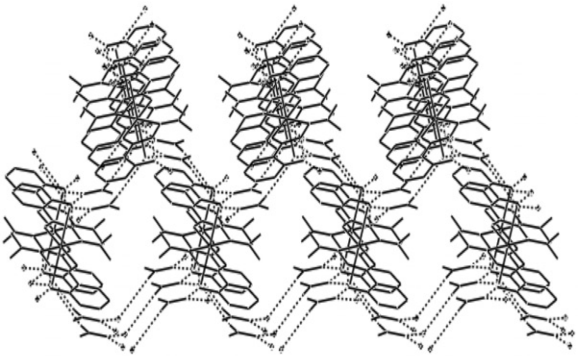

Figure 4. Cell packing of **2**.

Table 2. Selected bond lengths (Å) and angles (°).

1		**2**	
Ni–N1	2.133(3)	Ni–N1	2.135(2)
Ni–N3	2.146(5)	Ni–O1	2.057(2)
Ni–N4	2.132(4)	Ni–O2	2.0223(16)
Ni–O1	2.002(3)	C4–N2	1.3363(3)
C7–N2	1.331(5)	N1–N2	1.388(3)
N1–Ni–O1	101.22(11)	N1–Ni–O2	78.85(7)
N1–Ni–N1A	178.98(14)	N1–Ni–O1	87.24(8)
N1–Ni–N3	89.49(7)	N1–Ni–N1A	180.00(11)

bonded to Ni(II) similarly to that shown in **1**, but the pyridines in **1** are replaced by waters in **2**. The Ni–N bond lengths are from 2.132(4) to 2.146(5) Å for **1** and 2.135(2) Å for **2**. Similar observations have been reported for symmetrical mononuclear Ni(II) complexes [13, 14]. There are two types of Ni–N bonds in **1**, while **2** possesses

Table 3. Hydrogen bonding geometry (Å, °) of **1** and **2**.

D–H···A (Å)	D–H (Å)	H···A (Å)	D···A (Å)	D–H···A (°)
1				
N2–H2···O2	0.86	1.89	2.575(5)	135.5
O2–H2A···N2	0.82	1.91	2.575(5)	137.0
2				
N2–H2···O3	0.86	1.88	2.563(3)	135.6
O3–H3···O6	0.82	1.80	2.614(3)	171.3
O3–H3···N3	0.82	2.61	3.352(3)	151.1
O1–H1D···O5	0.80	2.04	2.827(3)	172(3)
O1–H1D···N3	0.80	2.63	3.397(4)	162(3)
O1–H1E···O6	0.80	1.95	2.747(3)	174(3)

only one. The mean value of Ni–N bond length is longer than that of Ni–O, which means oxygen has better coordination ability to Ni(II) than nitrogen. The C7–N2 bond lengths in **1** and C4–N2 in **2** are 1.331(5) and 1.3363(3) Å, respectively, such C–N bonds are multiple bonds. In **1** and **2**, nitrates are not coordinated to nickel.

The significant difference between the two complexes is the hydrogen-bonding pattern. In **1**, the complex contains two ligands and two pyridines, but in **2**, the complex contains two ligands and two waters. In **1**, each mononuclear unit is unassisted, the crystal structure is stabilized by intramolecular hydrogen bonds, (2.575(5) Å, 135.5°)N2–H2···O2 and (2.575(5) Å, 137.0°)O2–H2A···N2. In **2**, the units are linked via a triple-hydrogen-bonding nitrate to form a network. As shown in figure 4, the nitrates form hydrogen bonds through oxygens of nitrate with three adjacent hydroxyl and water oxygens of three different units (2.614(3) Å, 171.3°)O3–H3···O6, (2.747(3) Å, 174(3)°)O1–H1E···O6, and (2.827(3) Å 172(3)°)O1–H1D···O5. Intramolecular hydrogen bonds, (2.563(3) Å, 135.6°)N2–H2···O3, (3.352(3) Å, 151.1°)O3–H3···N3, and (3.397(4) Å, 162(3)°)O1–H1D···N3 play an important role in the stability of **2**.

3.2. *Formation of the complexes*

The original ligand $C_{15}H_{12}O_4N_2$ and the $Ni(NO_3)_2 \cdot 6H_2O$ first synthesized (scheme 1) is not stable complex **a**. Then, the *o*-carboxybenzaldehyde in complex **a** was replaced by acetone, without breaking coordination bonds and, more stable complex **b** was produced. Such reaction was also found in the literature [15].

3.3. *IR spectra*

IR spectra of these complexes and ligand exhibit several characteristic bands. In free ligand, the band at 1606 cm^{-1} is attributed to ν(C=N), which shifts to 1537 and 1548 cm^{-1} for **1** and **2**, respectively, due to the coordination by nitrogen of imine. The absorption of the free ligand at 1662 cm^{-1} is assigned to ν(C=O), which shifts to 1594 and 1620 cm^{-1} for **1** and **2**, respectively, showing the coordination of oxygen of carbonyl [16, 17]. In **1**, the band at 2700 cm^{-1} belongs to nitrogen of pyridine, coordinated to Ni(II). In **2**, the band at 3226 cm^{-1} is assigned to oxygen of water,

Table 4. Thermal decomposition data for **1** and **2** ($\beta = 10^{\circ}\mathrm{C\,min}^{-1}$).

	Stage I		Stage II		Stage III	
Complex	Temperature range (°C)	Weight loss (%)	Temperature range (°C)	Weight loss (%)	Temperature range (°C)	Weight loss (%)
1	100 ~ 228	22.00(21.80)	228 ~ 404	28.85(25.94)	404 ~ 800	28.02(27.32)
2	30 ~ 135	6.44(7.98)	135 ~ 452	49.29(50.10)	452 ~ 800	25.50(13.94)

coordinated to Ni(II). A strong band at $1380\,\mathrm{cm}^{-1}$ in **1** and **2** indicates that the ligand has changed.

3.4. *Thermal analysis*

The weight losses and the corresponding temperature ranges during the decomposition at heating rates of 5, 10, and $15^{\circ}\mathrm{C\,min}^{-1}$ are listed in table 4. The TG-DTG curves show that the thermal decomposition of **1** has three stages. The first is connected with the loss of pyridine from 100°C to 228°C with a mass loss of 22.00% (Calcd 21.80%). The second decomposition stage is the loss of phenol in the range 228–404°C with a mass loss of 28.85% (Calcd 25.94%). The third decomposition stage occurs from 404°C to 800°C assigned to the loss of five-membered chelate rings and gem-dimethyl groups with a mass loss of 28.02% (Calcd 27.32%). The remainder is NiO.

Thermal decomposition of **2** occurs at three stages. The first at 30–135°C with a mass loss of 6.44% (Calcd 7.98%) is assigned to the loss of water. The second stage from 135°C to 452°C with a mass loss of 49.29% (Calcd 50.10%) is assigned to loss of phenol and five-membered chelate rings. The third decomposition stage takes place from 452°C to 800°C with a mass loss of 25.50% (Calcd 13.94%) assigned to the loss of gem-dimethyl groups. The remainder is NiO.

3.5. *DNA binding study*

Before adding CT-DNA to **1** and **2**, their behavior in a buffer solution at room temperature was monitored by UV-Vis spectroscopy. Liberation of L^{-1} was not observed under these conditions, suggesting that the complexes are stable under the conditions.

The UV-Vis spectra of **1** and **2** with CT-DNA were done in Tris buffer from 500 nm to 200 nm. For **2**, a distinct charge transfer band appeared at 300 nm (figure 5b). This band upon addition of successive amounts of CT-DNA (0–50 µM) showed a small blue shift to 298 nm. For **1** (figure 5a), a blue shift is not very clear.

As reported previously [18], a change in band intensity upon the addition of DNA to metal complexes implies the interaction of the complexes with DNA base pairs, so we conclude that the complexes interact with DNA double strands; interaction of **2** with DNA is stronger than **1**. Comparing the DNA experimental phenomena with other Ni(II) complexes [19, 20], the complexes **1** and **2** have weak interaction, indicating possible groove binding and electrostatic actions [21].

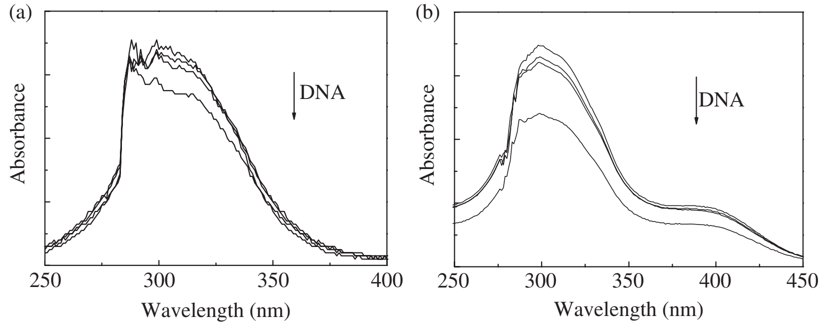

Figure 5. Changes in the absorption spectra of **1** (a) and **2** (b) on titration with increasing CT-DNA concentration (0–50 μM).

Table 5. The catalytic properties for decomposition of hydrogen peroxide.

Compounds	Decomposition percent of H_2O_2 (%)
$Ni(NO_3)_2 \cdot 6H_2O$	80.5
$C_{15}H_{12}O_4N_2$	85
1	91.4
2	90.5

3.6. *The catalytic activity of the compounds*

Catalytic decomposition activity to hydrogen peroxide showed that **1** and **2** have good catalytic activity (table 5). In the same concentration of catalyst, metal salts, and their complexes have catalytic decomposition activity. The ligand also has some catalytic activity. The complexes' catalytic performance is much better than the corresponding salts and ligand, and **1** has the best catalytic effect.

4. Conclusion

Ni(II) complexes have been synthesized and characterized, as mononuclear with Ni(II) octahedrally coordinated by ligands and solvent. The nitrate is not coordinated. The original ligands changed in the synthesis. Thermal decomposition of the complexes can be divided into three stages, and the thermal stability is **1** > **2**. Complex **2** has stronger interaction with DNA than **1**. Catalytic decomposition to hydrogen peroxide showed that **1** has the best catalytic effect.

Supplementary materials

CCDC 737715, 733608 contain the supplementary crystallographic data for **1** and **2**, respectively. These data can be obtained free of charge from the Cambridge Crystallographic Data Centre via http://www.ccdc.cam.ac.uk/conts/retrieving.html.

Acknowledgments

Financial support from the Special Education Fund of Shaanxi Province under grant No. 07JK317 is gratefully acknowledged.

References

[1] X.Z. You, Q.J. Meng, W.S. Han. *Progress in Coordination Chemistry*, Higher Education Press, Beijing (2006).
[2] Y.X. Ren, S.P. Chen, S.L. Gao. *J. Coord. Chem.*, **59**, 2135 (2006).
[3] K.M. Ibrahim, I.M. Gabr, R.R. Zaky. *J. Coord. Chem.*, **62**, 1100 (2009).
[4] Y.L. Song, Y.T. Li, Z.Y. Wu. *J. Inorg. Biochem.*, **102**, 1691 (2008).
[5] Y.G. Li, D.H. Shi, H.L. Zhu, H. Yan, S.W. Ng. *Inorg. Chim. Acta*, **360**, 2881 (2000).
[6] E.P. Zhang, H.W. Hou, H.Y. Han, Y.T. Fan. *J. Organomet. Chem.*, **693**, 1927 (2008).
[7] I.M. Gabr. *J. Coord. Chem.*, **62**, 3206 (2009).
[8] G.W. Yang, X.P. Xia. *Chin. J. Appl. Chem.*, **12**, 13 (1995).
[9] G.W. Yang, D.F. Wang. *Chem. Res. Chin. Univ.*, **16**, 55 (1995).
[10] J.C. Xian, R.T. Li, G.W. Cao, H.K. Lin, S.R. Zhu. *Chin. J. Inorg. Chem.*, **16**, 833 (2000).
[11] L.H. Bryant Jr, A. Lachgar, K.S. Coates, S.C. Jackels. *J. Inorg. Chem.*, **33**, 2219 (1994).
[12] L.Z. Meng, Y.B. He. *Analysis of Orag-amcspectrum*, Wuhan University Press, Wuhan (1997).
[13] M. Padmanabhan, J.C. Joseph, X.Y. Huang, J. Li. *J. Mol. Struct.*, **885**, 36 (2008).
[14] M.C.F. Fernandez, R. Bastida, A. Macias, P.P. Lourido, L. Valencia. *Polyhedron*, **28**, 2371 (2009).
[15] F. Yang, J.J. Lin, Y.K. Shan. *Coordination Chemistry*, East China Normal University Press, China (2002).
[16] F. Karipcin, B. Dede, S.P. Ozkorucuklu, E. Kabalcilar. *Dyes Pigm.*, **84**, 14 (2010).
[17] N.K. Singh, M.K. Bharty, R.J. Butcher. *Polyhedron*, **28**, 2443 (2009).
[18] H.P. Yang, W.H. Zhang, Q.X. Zhao, J.Y. Cai. *Chin. J. Inorg. Chem.*, **22**, 488 (2006).
[19] C.Y. Gao, X.F. Ma, J.L. Tian, D.D. Li, S.P. Yan. *J. Coord. Chem.*, **63**, 115 (2010).
[20] G.B. Bagihalli, S.A. Patil. *J. Coord. Chem.*, **62**, 1690 (2009).
[21] W.T. Wu. Structure, bioactivity and initial interaction research with DNA of complexes with aryl-acylhdrazone containing carboxylic acid, PhD thesis, Northwest University (2007).